Kochi Chapter

Indian Geotechnical Conference
IGC 2022
15th – 17th December, 2022, Kochi

Interaction Effects for Large Piled Rafts in Clay Soil

Rajib Modak[1] and Baleshwar Singh[2]

[1] Research Scholar, Department of Civil Engineering, Indian Institute of Technology Guwahati, Guwahati-781039, E-mail: rmodak@iitg.ac.in
[2] Professor, Department of Civil Engineering, Indian Institute of Technology Guwahati, Guwahati-781039, E-mail: baleshwar@iitg.ac.in

Abstract. The behavior of a piled raft foundation (PRF) depends on complex raft-soil-pile interactions. In the present paper, the effects of pile number, pile spacing, pile length, and pile diameter on the settlement-dependent variation of raft-soil-pile interactions and load-sharing behavior of large PRFs in clay soil have been evaluated. Three-dimensional numerical analyses were performed on different foundation types such as piled raft, unpiled raft, pile group, and single pile. Results show that the piles to piles (P-P) interaction effect approaches unity at a particular settlement value, and the value is larger for a higher pile number, pile length, and pile diameter. With the same number of piles, at higher settlement levels, the raft to piles (R-P) interaction effect is slightly larger at wider pile spacing. An insignificant effect in the settlement-dependent variation of the R-P interaction effect is observed for variation in pile number, pile length, and pile diameter. The piles to raft (P-R) interaction effect firstly decreases within initial settlement range and then increases as PRF settlement increase. The proportion of load carried by piles in PRF initially increases and then decreases with PRF settlement. The settlement at which the pile load proportion reaches a peak is larger for a higher pile number, pile length, and pile diameter.

Keywords: Large piled rafts; Numerical modeling; Interaction effects; Load-sharing; Pile group; Unpiled raft.

1 Introduction

In general the foundations types that are commonly in use are shallow (raft) and deep (pile) foundations. However, in recent decades a composite structure called piled raft foundation (PRF) consisting of both raft and piles has gained significant recognition. The PRF has proven to be a cost-effective foundation option compared to the traditional foundations to carry heavy superstructure loads due to the contribution of both raft and piles that are taken into account in the PRF design. Several practical examples of PRFs have been reported in the literature [1, 2]. The PRFs can be classified into two types, *i.e.*, small and large piled rafts [3]. In the case of small piled rafts, the width of raft (B_r) is smaller than the pile length (L_p) ($B_r/L_p < 1$). However, in the case of large piled rafts, the width of raft is greater than the length of piles ($B_r/L_p > 1$). As both the raft and piles in a PRF contribute to the load-sharing, a major design concept is the proportion of load carried by each structural element [4].

The overall load response of a PRF is governed by the complex interaction effects involved in the load-sharing mechanism, as shown in Fig. 1a. The interactions are

caused due to the overlapping of stress and displacement fields of individual structural elements (raft and piles). The different interaction effects of a PRF are: (1) piles to piles (P-P); (2) raft to piles (R-P); and piles to raft (P-R) [5]. The P-P interaction effect is the changes in the load response of pile group (PG) and single pile (SP). The R-P interaction effect represents the changes in the load response of PG due to the raft in PRF. The P-R interaction effect signifies the changes in the raft load response due to the piles in PRF. Taking into account the PRF interactions (Fig. 1a), Park and Lee [6] expressed the load carrying capacity of a PRF as follows:

$$Q_{\mathrm{pr}} = \alpha_{\mathrm{r}} Q_{\mathrm{ur}} + \alpha_{\mathrm{p}} Q_{\mathrm{pg}} = \alpha_{\mathrm{r}} Q_{\mathrm{ur}} + \alpha_{\mathrm{p}} \eta_{\mathrm{p}} Q_{\mathrm{sp}} \quad (1)$$

where η_{p}, α_{p}, and α_{r} are the P-P, R-P, and P-R interaction effects; Q_{ur}, Q_{pg}, and Q_{sp} are the load carrying capacities of unpiled raft (UR), PG where the raft is not in contact with the ground, and SP, respectively.

Several investigations on evaluating the PRF interactions have been reported in the literature [6 – 11]. Furthermore, studies on the load-sharing behavior of piled rafts have also been reported [12 – 15]. For PRFs in sand, centrifuge tests were carried out Park and Lee [6] and they found that both P-R and R-P interaction effects initially decreased and then increased with the increase in settlement. Halder and Manna [8] conducted experimental investigations on PRF in sand and suggested equations for calculating various PRF interactions. Kumar and Choudhury [10] carried out 3D FE analysis for PRFs in sand and proposed expressions for determining the bearing capacity using PRF interactions. Reul [11] carried out three-dimensional (3D) finite element (FE) analysis of PRF in overconsolidated clay and reported that at a higher load level due to PRF interactions, pile skin friction increases. Bhaduri and Choudhury [12] presented a displacement-based FE approach to evaluate the load-sharing behavior of PRF. Lee *et al.* [15] studied the load-settlement response of PRFs in clay experimentally and suggested a load-sharing model based on PRF settlement. However, most investigations on PRF interactions and load-sharing behavior were expressed as a function of foundation geometry and property conditions. A few literature have reported the effect of settlement on the interactions and load-sharing behavior of large PRF in stiff clay through numerical modeling. Thus in the present paper, the settlement-dependent variation of PRF interactions and the load-sharing behavior are evaluated for large PRFs in stiff clay soil with varying pile number, pile spacing, pile length, and pile diameter. For this purpose, 3D FE analyses have been performed using Plaxis 3D software [16].

2 3D Numerical Modeling

2.1 Boundary Conditions, Meshing and Soil Modeling

The drained soil behavior is considered and water table is assumed to be at ground surface. Based on the domain analysis study, the soil domain boundaries were considered large enough to avoid boundary effects (Fig. 1b). The domain of soil in the lateral directions is extended up to a distance equivalent to twice of the width of raft (B_{r}) from the edges of raft, with displacements allowed in vertical direction and restrained in horizontal direction. The bottom of the soil domain is extended up to thrice the length of pile (L_{p}) from the tip of pile, with displacements restricted in both directions (vertical

and horizontal). The ground surface displacements are free in all directions. To determine the optimum mesh size, mesh convergence study has been performed, and "Fine" mesh is selected. A finer mesh has been generated nearby the raft and piles by applying local mesh refinement. Fig. 1b illustrates the soil domain finite element mesh.

The Hardening soil model that is based on stress-dependent stiffness of soil is used to model the elasto-plastic soil behavior. This is an advanced soil model which includes both compression and shear hardening. Three input parameters are required to represent the elastoplastic soil deformation, *i.e.*, ref. secant stiffness modulus (E_{50}^{ref}), ref. oedometer stiffness modulus ($E_{\mathrm{oed}}^{\mathrm{ref}}$), and ref. unloading-reloading stiffness modulus ($E_{\mathrm{ur}}^{\mathrm{ref}}$) (Table 2). The different stress-dependent stiffnesses (E) are estimated using Eq. 2.

$$E = E^{\mathrm{ref}} \left(\frac{c' \cot \emptyset' + \sigma'}{c' \cot \emptyset' + p^{\mathrm{ref}}} \right)^{m} \tag{2}$$

where E^{ref} is the reference stiffness value corresponding to the reference stress (p^{ref}) level of 100 kPa, σ' is the stress level, c' and ϕ' are the shear strength parameters, and m is the stress dependency factor.

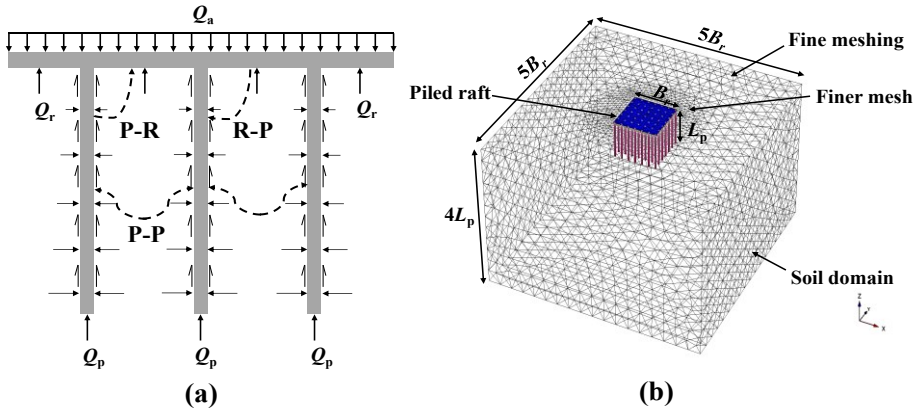

Fig. 1. (a) Load-sharing mechanism and PRF interactions; (b) Typical FE mesh of the soil domain and PRF.

2.2 Validation

The validation of the present study is performed by comparing the load-settlement variations of PRFs as indicated by Cho *et al*. [17]. The finite element software Abaqus was by Cho *et al*. [17] and for the soil modeling, Mohr-Coulomb model has been employed. A 10 x 10 m and 1 m thick raft with nine piles arranged in 3 x 3 square pattern of 0.5 m diameter, with spacing equivalent to thrice the diameter of pile and length of piles of 8 and 16 m is selected. The properties of the materials are given in Table 1. As shown in Fig. 3, the results obtained from the present study are in good agreement with the reported results.

Table 1. Material properties [17].

	Clay (stiff)	Bearing layer	Raft	Piles
Elasticity modulus, E'(MPa)	45	500	30,000	12,500
Cohesive strength, c'(kPa)	20	0.1	-	-
Angle of friction, ϕ'(°)	20	45	-	-
Poisson's ratio, ν'	0.3	0.3	0.2	0.25
Total unit weight, γ_t (kN/m^3)	19	20	25	25

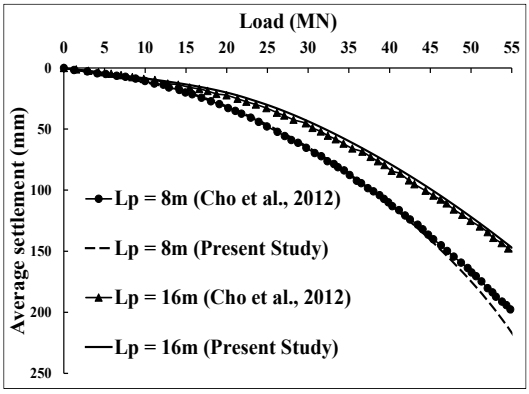

Fig. 2. Load-settlement behavior of Plaxis 3D compared with Cho *et al*. [17].

3 Numerical analyses

3.1 Piled raft interactions and load-sharing

A squared raft of 38 x 38 m size [18] and 2 m thickness has been considered for the numerical analyses. The particular raft thickness corresponds to that of an intermediate flexible raft based on the raft-soil stiffness ratio [19]. Table 2 presents the soil [20], raft [18], and pile [18] properties used for the study. Three different PRF interaction effects, as mentioned in Section 1 are considered, *i.e.*, piles to piles (P-P), raft to piles (R-P), and piles to raft (P-R) effect. The settlement-dependent variation of these interactions has been evaluated for the variation in the number of piles, spacing between piles, length of piles, and diameter of piles (Table 3). The number of piles (N_p) vary from 25 to 81 piles such that the area enclosed by the pile group (B_g), as shown in Fig. 3, is the same for all the PRFs. For 49 piles, the pile spacing (s) is varied from minimum to maximum possible pile spacing. The minimum pile spacing as per IS 2911 Part 1 [21] for group piles in clay soil is three times the pile diameter (D_p). For the same 49 piles, the pile length (L_p) is now varied between 20 to 30 times the diameter (D_p) of the pile. Again for 49 piles, the pile diameter is varied from 0.5 m to 1.5 m. In the study, while varying one parameter, the standard values (Table 3) of all the other parameters are considered. In addition to the PRF models, corresponding load-settlement responses of UR, PG, and SP are also analyzed to evaluate the different PRF interactions. The settlement-dependent variation of the P-P interaction effect is obtained by evaluating the ratio of load capacity of PG (with 'N_p' number of piles) to the load capacity of 'N_p' SP

at the same settlement level. For R-P interaction effect, the ratio of the load capacity of piles in PRF to the PG load capacity with a similar number of piles as PRF is calculated. Furthermore, to determine the variation of P-R interaction effect with PRF settlement, the ratio of the load capacities of the raft in a PRF to that of the UR is evaluated.

The study considers a settlement criteria of 0.35% B_r [14]. The settlement-dependent variation of the PRF interactions is observed up to the maximum average settlement (w_{avg}) of 0.35% B_r. Thus, all the foundations are subjected to a load corresponding to which w_{avg} is equivalent to 0.35% B_r. A uniformly distributed load (*UDL*) over the raft area is applied in the case of UR, PG, and PRF, whereas for SP, point load at the pile head is applied to determine the load-settlement response. The w_{avg} is evaluated using Eq. 3 [18], where w_{center} and w_{corner} are the raft's center and corner settlements, respectively. To understand the variation in the load-sharing behavior of PRF with settlement, the percentages load shared by raft and piles are evaluated. The pile load share is evaluated as the sum of axial load at all pile heads, and the raft load share is then obtained by deducting the pile load share from the total applied load.

$$w_{\text{avg}} = \frac{1}{3}(2w_{\text{center}} + w_{\text{corner}}) \tag{3}$$

Table 2. Material properties of soil, raft, and piles.

Materials	Properties	Values
Soil	Unit weights γ_{unsat}/ γ_{sat} (kN/m^3)	20/20
	Poisson's ratio, v_s	0.2
	Cohesion, c' (kN/m^2)	20
	Angle of friction ϕ' (°)	20
	Coefficient of lateral earth pressure (K_o)	0.8
	Ref. secant stiffness modulus, E_{50}^{ref} (kN/m^2)	3.50 x 10^4
	Ref. oedometer stiffness modulus, E_{oed}^{ref} (kN/m^2)	4.28 x 10^4
	Ref. unloading-reloading stiffness modulus, E_{ur}^{ref} (kN/m^2)	1.05 x 10^5
	Stress dependency power, m	1
Raft	Unit weight (kN/m^3)	25
	Elastic modulus, E_r (MN/m^2)	34,000
	Poisson's ratio, v_r	0.2
Piles	Unit weight (kN/m^3)	25
	Elastic modulus, E_p (MN/m^2)	30,000
	Poisson's ratio, v_p	0.2

Table 3. Piled raft geometric configurations.

Parameters	Values
Width of raft, B_r (m)	38
Thickness of raft, t_r (m)	2
Pile number, N_p	25, 49*, 81
Pile spacing, s (m)	3, 4, 5, 6*,
Pile length, L_p (m)	20, 25, 30*
Pile diameter, D_p (m)	0.5, 1*, 1.5

* Standard value if not varied.

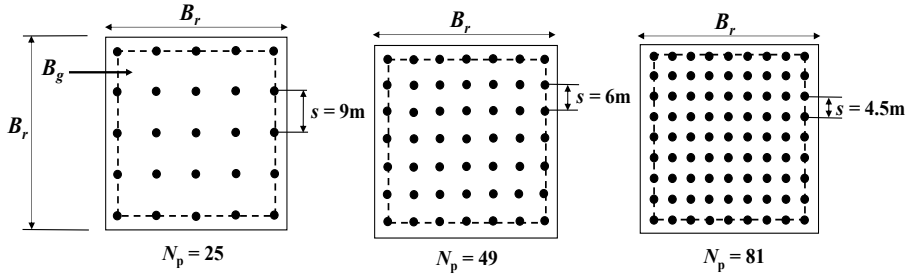

Fig. 3. Various pile configurations used in the study.

3.2 Results and Discussion

Influence of pile number. The influence of pile number on the settlement-dependent variation of the PRF interactions and the load-sharing behavior is presented in Fig. 4. Fig. 4a shows that for all the pile configurations, *i.e.*, 5 x 5, 7 x 7, and 9 x 9, the P-P interaction effect (η_p) is lower within the initial settlement range and it approaches a constant value of unity at a higher settlement value. This implies piles in PG having a lower load capacity than 'N_p' SP within the initial settlement range and this is due to greater overlapping of stresses and displacement fields within the piles in PG. Also, within the initial settlement range, the η_p value is lower for a higher number of piles. However, as PRF settlement increase, once the capacity of piles in PG is mobilized fully, η_p approaches unity for all the pile configurations. The settlement value corresponding to which the $\eta_p \approx 1$ is larger for a higher pile number. de Sanctis and Mandolini [7] suggested adopting a η_p of unity based on FE analysis results for PRF in soft clay deposits. The R-P interaction effect (α_p) influences the load response of PRF in two ways, *i.e.,* positive and negative. The positive aspect corresponds to the fact that due to the raft's presence, the confining stress of soil underneath the raft increases, which further increases the pile skin friction resistance. The negative aspect is related to the lesser relative pile-soil displacement due to the downward movement of the soil underneath the raft upon loading. Fig. 4b shows the settlement-dependent variation of α_p for different pile numbers. For all the pile configurations, almost a similar trend of α_p variation with PRF settlement is observed. The negative effect is encountered initially, but with the increase in settlement, the positive effect is more pronounced. At the maximum settlement of 0.35% B_r (≈ 135 mm), the α_p values for piles varying from 25-81 lie within a close range of 1.0-1.04.

The P-R interaction effect (α_r) indicates the changes in the load-settlement response of the raft due to the presence of piles underneath in PRF. The variation of α_r with respect to PRF settlement for varying pile numbers is shown in Fig. 4c. The figure illustrates that, for all the pile configurations, α_r decreases initially and then gradually increases with the increase in the settlement. The initial decrease is because of the reduction of raft-soil contact pressure due to the downward soil movement. However, with the increase in settlement, once the pile capacity of piles in PRF is fully mobilized, the raft contribution in PRF increases, and thus α_r increases. Park and Lee [6] have also reported similar results by means of centrifuge tests conducted for PRF in sands. Moreover, the α_r values are lower for a higher number of piles due to lower raft-soil contact pressure. The α_r value at the maximum settlement of 0.35% B_r range from 0.48-0.92 for

piles varying from 81-25, respectively. The load-sharing behavior in terms of percentage of load carried by each structural element at different settlement levels for varying pile numbers is shown in Fig. 4d. It can be seen that with the increasing pile number, the pile load share increases, and that of the raft decreases. For any pile number, the pile load share increases to a certain settlement value and then decreases with the increasing PRF settlement. The settlement values at which the dip in the pile load share is observed for all pile configurations are similar to the settlements at which η_p approaches unity and α_r increases after showing a decreasing trend. The settlement values for which a decrease in pile load share is encountered for 25, 49, and 81 piles are 30, 55, and 75 mm, respectively. This shows that at these settlements, the pile capacity of piles in PRF is fully mobilized, and further increment in load is carried by the raft.

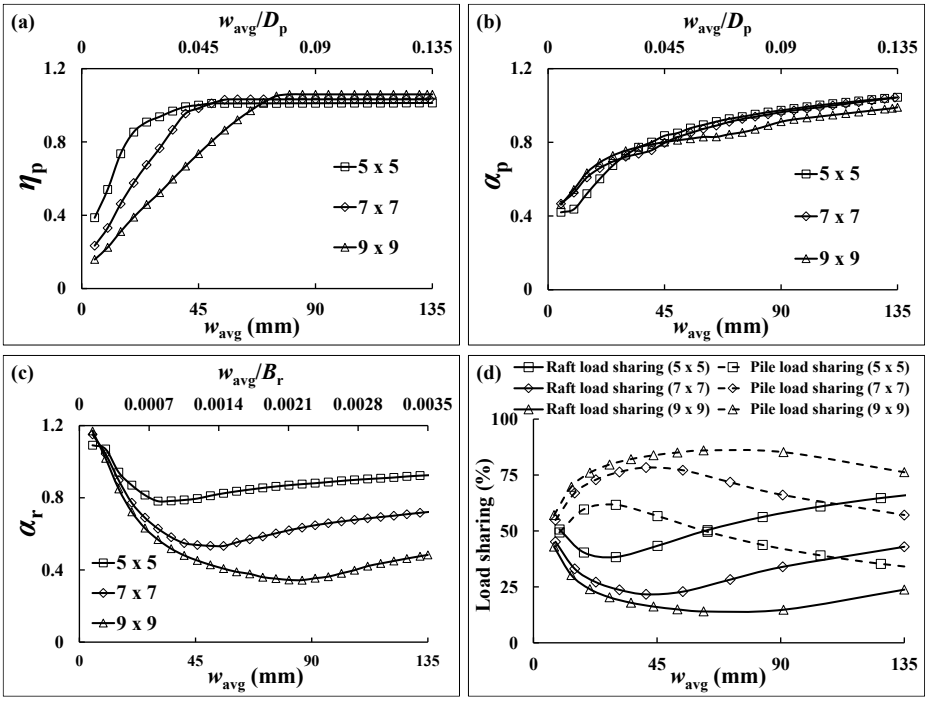

Fig. 4. Influence of pile number on PRF interactions and load-sharing behavior.

Influence of pile spacing. Fig. 5 shows the influence of pile spacing on PRF interactions and load-sharing behavior variation with settlement. The standard 7 x 7 pile configuration with different s/D_p (pile spacing to pile diameter) ratios of 3, 4, 5, and 6 are considered. For the different s/D_p ratios considered, a lower η_p value is observed initially, and then it approaches unity at a higher settlement level, as shown in Fig. 5a. Also, within the initial settlement range, the η_p value is higher for a larger s/D_p ratio. The reason is at a larger s/D_p ratio the stress and displacement fields overlapping decreases, and the pile behavior in PRF is similar to that of SP. The figure also shows that the PRF settlement corresponding to which $\eta_p \approx 1$ is lower for a larger pile spacing. The variation of α_p with PRF settlement for varying pile spacing is presented in Fig. 5b. It can be observed that for all s/D_p ratios, the negative effect is significant initially, followed by the positive effect at a higher settlement value. In addition, the α_p variation is

almost similar initially at the lower settlement range, and at a higher settlement level the α_p value is slightly greater for a larger s/D_p ratio. The α_p value lies within the range of 0.9-1.04 at the settlement of 0.35% B_r for s/D_p ratio varying from 3-6, respectively.

The settlement-dependent variation of α_r for varying s/D_p ratios is shown in Fig. 5c. The figure shows α_r decreases continuously for smaller s/D_p ratios (3 and 4) up to the maximum settlement of 0.35% B_r. However, for larger s/D_p ratios (5 and 6), the α_r value initially decreases and then increases with the increase in PRF settlement. This is because at a smaller s/D_p ratio due to greater superimposition of stresses and displacement fields, the pile capacity is not fully mobilized within the considered settlement range. The α_r value at 0.35% B_r settlement lies within the close range of 0.68-0.75 for the different s/D_p ratios considered. Fig. 5d illustrates the load shared by the piles and raft in PRF at different s/D_p ratios. With the increase in the pile spacing, the pile load share increases, and that of the raft decreases. This is because, with the increase in pile spacing, the pile behavior in PRF is comparable to SP as no neighbouring piles influence is experienced. However, it can be observed that the increase in the pile load share is not that significant for the increase in s/D_p ratio from 5 to 6.

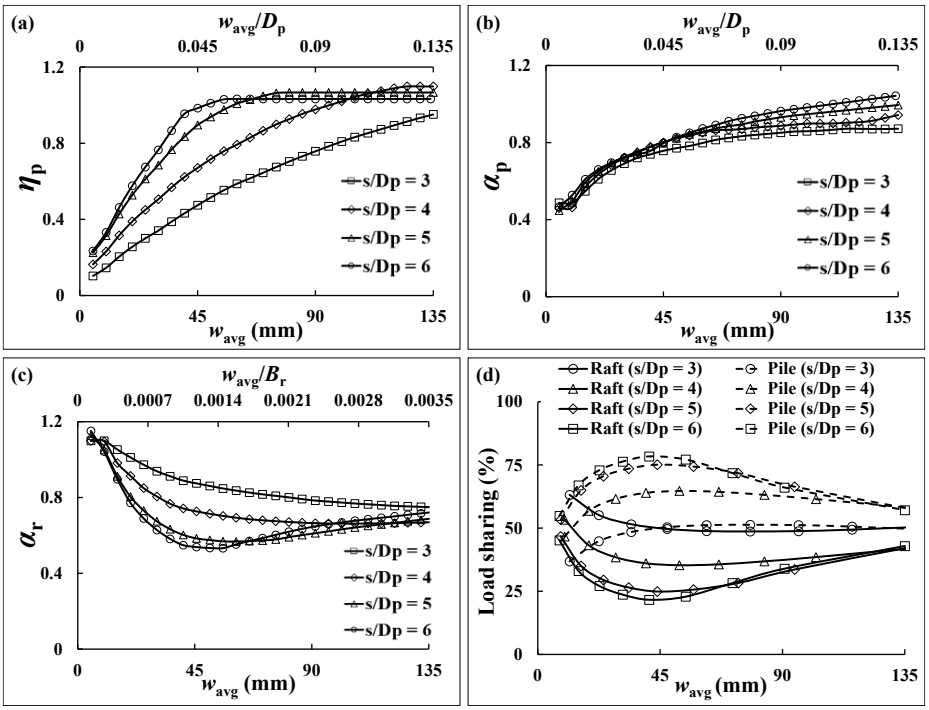

Fig. 5. Influence of pile spacing on PRF interactions and load-sharing behavior.

Influence of pile length. To understand the effect of pile length on the PRF interactions and load-sharing behavior, the 7 x 7 pile configuration with three pile length to pile

diameter ratios (L_p/D_p) has been considered, which are 20, 25, and 30. The other standard parameters have been selected from Table 3. Fig. 6a illustrates the variation of η_p with respect to settlement for different L_p/D_p ratios. The settlement value corresponding to which η_p approaches unity increases as the length of pile increase. This is because a higher settlement is required for the pile capacity to be fully mobilized for longer length piles. The settlement-dependent variation of α_p for PRFs with varying L_p/D_p ratios is shown in Fig. 6b. From the figure, it can be seen that a variation in the length of pile has insignificant effect on α_p variation with PRF settlement. The α_p value varies from 1.01-1.04 at the maximum settlement of 0.35% B_r for the L_p/D_p ratio varying from 20-30, respectively. The α_r value, as shown in Fig. 6c, initially decreases and then increases with the increase in PRF settlement for all L_p/D_p ratios considered. The decrease in α_r value is observed to be more significant for longer length piles. The minimum value of α_r (0.53) is encountered for the L_p/D_p ratio of 30 at the settlement of 50 mm. At the settlement of 0.35% B_r, the α_r value range from 0.72-0.85 for L_p/D_p ratios varying from 30-20, respectively. From the load shared by the individual structural elements, as shown in Fig. 6d, it can be seen that the pile load share increases with the increase in the pile length. This is due to the increase in the pile load capacity with the increasing length of piles in PRF. Furthermore, it can also be observed that the settlement value corresponding to which the raft load share rises and that of pile decreases, increases with the increase in the pile length.

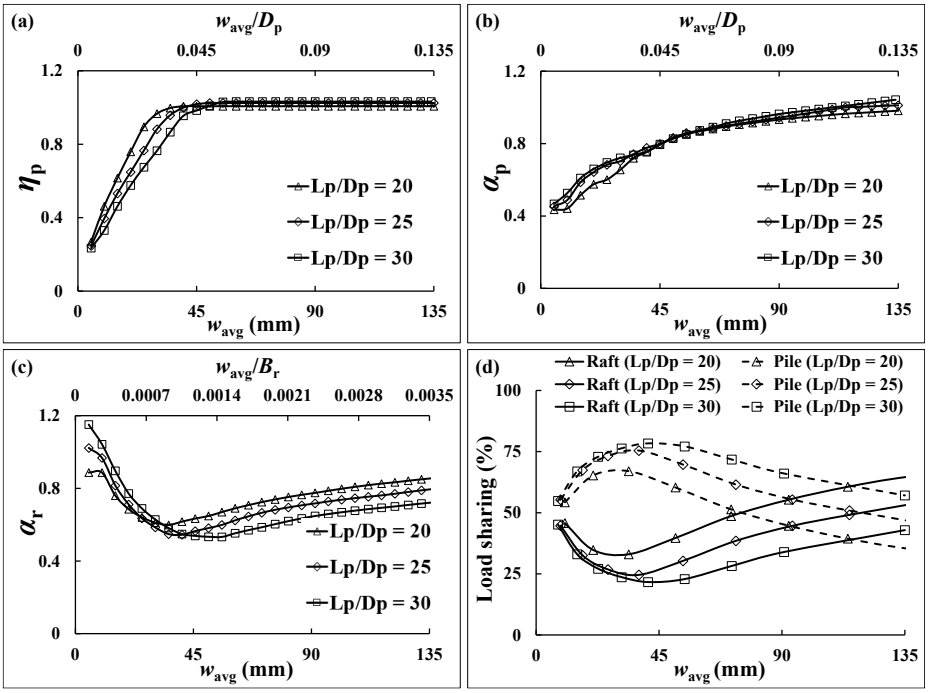

Fig. 6. Influence of pile length on PRF interactions and load-sharing behavior.

Influence of pile diameter. The standard 7 x 7 pile configuration is selected with pile diameter varying from 0.5-1.5 m to understand the effect of pile diameter on the settle-

ment-dependent variation of PRF interactions and load-sharing. For all the other parameters, the standard values are considered (Table 3). Fig. 7a presents the η_p variation with PRF settlement for different pile diameters. The η_p value is lower for larger diameter piles at the initial settlement range. The settlement value corresponding to which $\eta_p \approx 1$ increases with the increase in pile diameter. The α_p variation with settlement as shown in Fig. 7b shows no significant difference for the different pile diameters considered. However, within this range of settlement, up to 0.35% B_r the α_p value increases gradually with PRF settlement. The α_p value at 0.35% B_r settlement, range from 0.98-1.04 for the pile diameter varying from 1.5-0.5 m, respectively. The α_r variation with PRF settlement for varying pile diameters is shown in Fig. 7c. It can be observed that the α_r values significantly decrease as the pile diameter increases. This is because with increasing diameter the pile capacity increases, resulting in the reduction of raft contribution in PRF and thus α_r decreases. The minimum value of α_r (0.39) is observed in the case of PRF with piles of 1.5 m diameter and corresponding to the settlement of 65 mm. At the maximum settlement of 0.35% B_r, the α_r value ranges from 0.5-0.91 for pile diameter varying from 1.5-0.5 m, respectively. de Sanctis and Mandolini [7] have reported the range of α_r from 0.4 to 1.0 for PRF in soft clays. From the percentage load share, as shown in Fig. 7d, it can be seen that with the increase in the pile diameter the pile load share increases. Also, within the range of settlement considered, the piles carry the majority of the load except in the case of PRF with 0.5 m diameter piles. This can be attributed to full pile load capacity mobilization ofor smaller diameter piles at a lower settlement level.

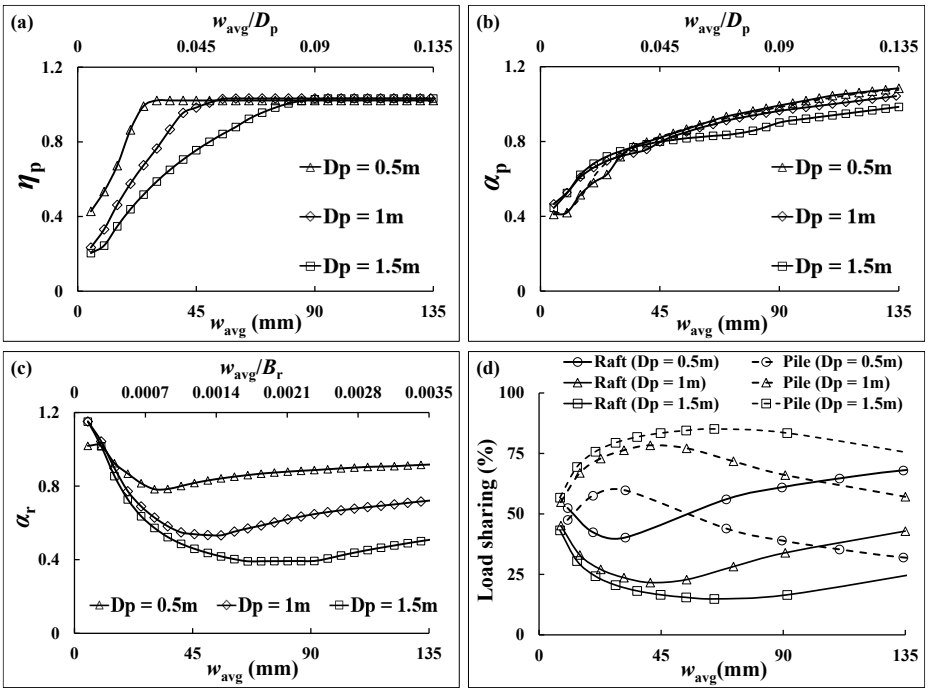

Fig. 7. Influence of pile diameter on PRF interactions and load-sharing behavior.

4 Conclusions

In the study, 3D numerical analyses were performed on large PRFs in stiff clay soil with varying pile number, pile spacing, pile length, and pile diameter to determine the settlement-dependent variation of PRF interactions and load-sharing behavior. The load-settlement responses of UR, PG, and SP were analyzed to evaluate the different PRF interactions. The P-P interaction effect approached unity at a higher settlement level for all the PRFs considered in the study. The settlement corresponding to which the P-P interaction effect reaches unity increased with the increase in pile number, pile length, and pile diameter, and it decreased with the increase in the pile spacing. In the scope of the study, the negative R-P interaction effect was observed initially and with the increase in the PRF settlement, the positive R-P interaction effect was more prevalent. No significant difference in the R-P interaction effect variation with respect to PRF settlement was observed for varying pile number, pile length, and pile diameter. However, at a settlement of 0.35% B_r, the R-P interaction effect is marginally higher for a larger pile spacing. The R-P interaction effect showed an increasing trend for all PRFs, and it ranged from 0.9-1.04 with an average of about 0.97 at the maximum average settlement of 0.35% B_r.

The P-R interaction effect initially decreased due to lower raft-soil contact stress and then increased as the pile capacity of the piles in PRF was fully mobilized. The settlement value up to which a decreasing trend in the P-R interaction effect was observed increased for a higher pile number, pile length, and pile diameter. However, for PRFs with a smaller pile spacing, the P-R interaction effect decreases continuously within the settlement range considered in the study. Overall the P-R interaction effect varied in the range from 0.48 to 0.92, with an average value of 0.7. From the load-sharing behavior, it was observed that the pile load share increased and that of raft decreased as pile number, spacing, length, and diameter increases for the entire settlement range considered. The pile load share initially increased with the PRF settlement and then decreased once the pile load capacity was fully mobilized. The settlement value at which the pile load share reaches a peak is greater for a higher pile number, length, and diameter.

References

1. El-Mossallamy, Y.: Innovative application of piled raft foundation in stiff and soft subsoil. In Deep Foundations 2002: An International Perspective on Theory, Design, Construction, and Performance, 426-440 (2002).
2. Poulos, H. G.: Piled raft foundations: Design and applications. Geotechnique, 51(2), 95-113 (2001).
3. Russo, G. & Viggiani, C.: (1998). Factors controlling soil-structure interaction for piled rafts. Darmstadt Geotechnics, 4, 297–321.
4. Clancy, P., & Randolph, M. F.: Simple design tools for piled raft foundations. Geotechnique, 46(2), 313-328 (1996).
5. Katzenbach, R., Arslan, U., & Moormann, C.: Piled raft foundation projects in Germany. Design applications of raft foundations, J. A. Hemsley, ed., Thomas Telford, London, 323–391 (2000).

6. Park, D., & Lee, J.: Interaction effects on load-carrying behavior of piled rafts embedded in clay from centrifuge tests. Canadian Geotechnical Journal, 52(10), 1550-1561 (2015).
7. de Sanctis, L., & Mandolini, A.: Bearing capacity of piled rafts on soft clay soils. Journal of Geotechnical and Geoenvironmental Engineering, 132(12), 1600-1610 (2006).
8. Halder, P., & Manna, B.: A new model for the prediction of load sharing in piled raft system-an experimental investigation. Arabian Journal for Science and Engineering, 46(11), 10667-10680 (2021).
9. Horikoshi, K., & Randolph, M. F.: A contribution to optimum design of piled rafts. Geotechnique, 48(3), 301-317 (1998).
10. Kumar, A., & Choudhury, D.: Development of new prediction model for capacity of combined pile-raft foundations. Computers and Geotechnics, 97, 62-68 (2018).
11. Reul, O.: Numerical study of the bearing behavior of piled rafts. International Journal of Geomechanics, 4(2), 59-68 (2004).
12. Bhaduri, A., & Choudhury, D.: Serviceability-based finite-element approach on analyzing combined pile–raft foundation. International Journal of Geomechanics, 20(2), 04019178 (2020).
13. Conte, G., Mandolini, A., & Randolph, M. F.: Centrifuge modelling to investigate the performance of piled rafts. Proc., 4th Int. Geotechnical Seminar on Deep Foundations on Bored and Auger Piles, W. F. Van Impe, ed., Millpress, Rotterdam, Netherlands, 359–366 (2003).
14. Lee, J., Kim, Y., & Jeong, S.: Three-dimensional analysis of bearing behavior of piled raft on soft clay. Computers and Geotechnics, 37(1-2), 103-114 (2010).
15. Lee, J., Park, D., & Choi, K.: Analysis of load sharing behavior for piled rafts using normalized load response model. Computers and Geotechnics, 57, 65-74 (2014).
16. Brinkgreve, R., Swolfs, W., & Engin, E.: PLAXIS user's manual, version 6.1. Balkema, Rotterdam, The Netherlands (2015).
17. Cho, J., Lee, J. H., Jeong, S., & Lee, J.: The settlement behavior of piled raft in clay soils. Ocean Engineering, 53, 153-163 (2012).
18. Reul, O., & Randolph, M. F.: Design strategies for piled rafts subjected to nonuniform vertical loading. Journal of Geotechnical and Geoenvironmental Engineering, 130(1), 1-13 (2004).
19. Fraser, R. A., & Wardle, L. J.: Numerical analysis of rectangular rafts on layered foundations. Geotechnique, 26(4), 613-630 (1976).
20. Engin, H. K., & Brinkgreve, R. B. J.: Investigation of pile behaviour using embedded piles. In Proc.of the 17th International Conf. on Soil Mechanics and Geotechnical Engineering, Alexandria, 1189-1192 (2009).
21. IS 2911–Part 1, Section 4: Design and construction of pile foundations–Code of practice, Bureau of Indian Standards (2010).